Author(s): Ranta, Mikaela & Hinkkanen, Marko

Title: Online identification of parameters defining the saturation characteristics of induction machines

Year: 2012

Version: Post print

Please cite the original version:

Ranta, Mikaela & Hinkkanen, Marko. 2012. Online identification of parameters defining the saturation characteristics of induction machines. 2012 XXth International Conference on Electrical Machines (ICEM). 7. ISBN 978-1-4673-0141-1 (electronic). DOI: 10.1109/icelmach.2012.6350002.

Online Identification of Parameters Defining the Saturation Characteristics of Induction Machines

Mikaela Ranta and Marko Hinkkanen
Aalto University School of Electrical Engineering
P.O. Box 13000, FI-00076 Aalto, Finland

***Abstract*—The induction machine model parameters need to be estimated with good accuracy to ensure a good performance of the drive. Due to the magnetic saturation, the inductances vary as a function of the flux level. The magnetizing curve can be identified at standstill, but more accurate results are obtained if the identification is performed as the machine is running. In this paper, the magnetic saturation is modelled using a power function, and adaptation laws for the function parameters are proposed. The adaptation method is implemented in the control system of a sensorless drive. Experimental results on a 2.2-kW machine show that the identification of the stator inductance is rapid and the accuracy is good.**

***Index Terms*—Induction motor, magnetic saturation, parameter estimation, sensorless control.**

I. Introduction

The control of an electric drive is based on a model of the machine. In order to achieve a good performance, the model parameters need to be identified with good accuracy. Particularly, when the flux-weakening region is entered or the flux is controlled in order to optimize the drive, for instance, a loss-minimizing algorithm is applied, the dependency of the inductances on the magnetic saturation should be known.

The magnetic saturation is commonly taken into account by modelling the magnetizing inductance as a function of the magnetizing flux or current. Hence, the saturation can be modelled with a rather simple function and the resulting inductance is accurate enough in most cases. In machines having closed or skewed rotor slots, the load might slightly affect the saturation characteristics due to partly common iron paths of the magnetizing and leakage fluxes [1], [2]. The phenomenon can be investigated by finite element analysis and by measurements in a laboratory environment where the speed and load can be freely varied. However, in real-life applications, the identification of the magnetizing curve becomes difficult if the influence of the load is taken into account.

A great number of different methods to identify the magnetic characteristics during the start up of the drive have been developed [3]–[6]. These methods can be applied at standstill and the load does not need to be disconnected. However, as stated in [5], a correction factor should be used to achieve the same accuracy as when three-phase supply is used. Identification methods at standstill are also prone to voltage measurement errors as low voltage levels have to be used. The magnetizing curve can also be identified as the machine is running without load [7]. To store the magnetizing curve, a look-up table can be used, or a function can be fitted to the data unless the function parameters are directly identified. It is also possible to update the inductance during the operation of the drive [8]. In this case, a magnetizing curve does not necessarily need to be stored in the memory. On the other hand, continuous adaptation of the inductance might lead to poor dynamic behaviour of the drive.

In this paper, the stator inductance is modelled as a function of the stator flux using a simple power function. A method to identify the power function parameters during the start up of a sensorless drive is proposed. By varying the flux as the machine is running, the parameters of the saturation function can rapidly be identified, and the stator inductance can be calculated in every operating point without using any additional data fitting method. As the correct function parameters are obtained, the adaptation mechanism can be turned off without losing control accuracy when the flux varies later on. Hence, good dynamic performance of the drive can be ensured. The adaptation method is combined with a leakage inductance identification method based on signal injections in order to ensure good results also when a no-load condition cannot be reached during the stator inductance identification process. Simulations and laboratory experiments are performed in order to investigate the proposed adaptation method. The results show that the convergence of the parameter estimates is fast and the accuracy is good.

II. Induction Machine Model

Real-valued space vectors will be used; for example the stator current is $\boldsymbol{i}_\mathrm{s} = \begin{bmatrix} i_\mathrm{sd} & i_\mathrm{sq} \end{bmatrix}^\mathrm{T}$ and its magnitude is denoted by

$$i_\mathrm{s} = \|\boldsymbol{i}_\mathrm{s}\| = \sqrt{i_\mathrm{sd}^2 + i_\mathrm{sq}^2} \tag{1}$$

The identity matrix is $\mathbf{I} = \left[\begin{smallmatrix} 1 & 0 \\ 0 & 1 \end{smallmatrix}\right]$ and the orthogonal rotation matrix is $\mathbf{J} = \left[\begin{smallmatrix} 0 & -1 \\ 1 & 0 \end{smallmatrix}\right]$. The induction machine can be described by the Γ model or the inverse-Γ model. In the following, the models are shortly presented as they both will be used in the observer.

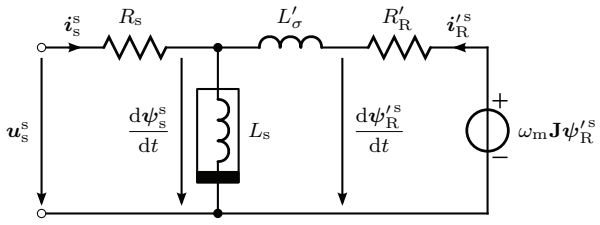

Fig. 1. Dynamic Γ model in stator coordinates. The superscript s denotes stator coordinates.

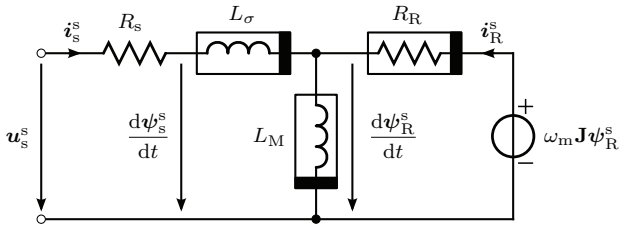

Fig. 2. Inverse-Γ model in stator coordinates.

A. Γ Model

In synchronous coordinates rotating at the angular frequency ω_s, the induction machine can be described by

$$\frac{d\boldsymbol{\psi}_s}{dt} = \boldsymbol{u}_s - R_s \boldsymbol{i}_s - \omega_s \mathbf{J}\boldsymbol{\psi}_s \tag{2a}$$

$$\frac{d\boldsymbol{\psi}'_R}{dt} = -R'_R \boldsymbol{i}'_R - \omega_r \mathbf{J}\boldsymbol{\psi}'_R \tag{2b}$$

where $\boldsymbol{u}_s$ is the stator voltage, $\boldsymbol{i}_s$ the stator current, and $\boldsymbol{i}'_R$ the rotor current. The stator flux is denoted by $\boldsymbol{\psi}_s$ and the rotor flux by $\boldsymbol{\psi}'_R$. The stator resistance and rotor resistance are R_s and R'_R, respectively. The angular slip frequency $\omega_r = \omega_s - \omega_m$, where ω_m is the electrical rotor speed. The stator flux and rotor flux are given by

$$\boldsymbol{\psi}_s = L_s(\boldsymbol{i}_s + \boldsymbol{i}'_R), \qquad \boldsymbol{\psi}'_R = \boldsymbol{\psi}_s + L'_\sigma \boldsymbol{i}'_R \tag{3}$$

where L_s is the stator inductance and L'_σ the leakage inductance. The Γ model is shown in Fig. 1.

B. Inverse-Γ Model

The magnetic saturation can easily be modelled in the Γ model, but the inverse-Γ model in Fig. 2 is more convenient in the control of the drive. In the inverse-Γ model, the flux equations are

$$\boldsymbol{\psi}_s = L_\sigma \boldsymbol{i}_s + \boldsymbol{\psi}_R, \qquad \boldsymbol{\psi}_R = L_M(\boldsymbol{i}_s + \boldsymbol{i}_R) \tag{4}$$

where L_σ is the leakage inductance and L_M the magnetizing inductance.

In steady state, the conversion between the two models can easily be done. For instance, if the parameters of the Γ model are known, the parameters of the inverse-Γ model are obtained as

$$L_M = \gamma L_s, \quad L_\sigma = \gamma L'_\sigma, \quad R_R = \gamma^2 R'_R \tag{5}$$

where

$$\gamma = \frac{L_s}{L_s + L'_\sigma} \tag{6}$$

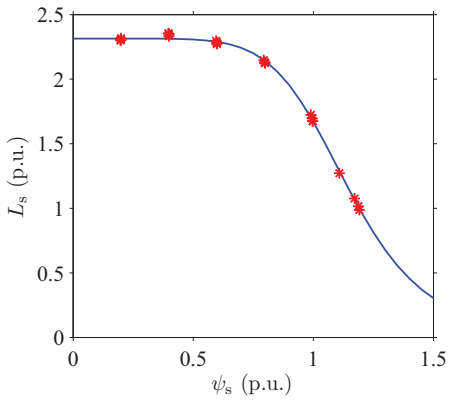

Fig. 3. Stator inductance as function of stator flux when $L_{su} = 2.31$ p.u., $\beta = 0.87$ p.u., and $S = 7$. Markers show the measured values from no-load tests on a 2.2-kW machine.

The expressions for the conversion are valid also during transients in the case of constant parameters, i.e. if the machine does not saturate.

C. Magnetic Saturation

The stator inductance and the leakage inductance depend on the flux linkages (or the currents) due to the magnetic saturation. In the case of the Γ model, modeling the stator inductance L_s as a function of the stator flux typically suffices. The leakage inductance L'_σ is assumed to be constant and the stator inductance is modeled by a simple power function [9]:

$$L_s = \frac{L_{su}}{1 + (\beta \psi_s)^S} \tag{7}$$

where L_{su} is the unsaturated inductance, and S and β are nonnegative constants. An example of the stator inductance is shown in Fig. 3. The model describes the saturation very well under no load. However, the load might affect the saturation characteristics in machines having skewed or closed rotor slots [10]. In other words, as the leakage flux increases, the stator inductance may decrease even though the stator flux remains the same. In this paper, the model in (7) is used since it has only three parameters. In Section IV-B, a method for identifying the parameters L_{su} and β is proposed, and S can be selected based on a priori information.

III. Observer

The reduced-order observer presented in [11] will be used, with the addition of adaptation of the stator inductance parameters L_{su} and β. The observer is based on the inverse-Γ model. Two back EMFs are used in the estimation of the rotor flux: the back EMF corresponding to the voltage model

$$\boldsymbol{e}' = \boldsymbol{u}_s - R_s \boldsymbol{i}_s - \hat{L}_\sigma \frac{d\boldsymbol{i}_s}{dt} - \hat{\omega}_s \hat{L}_\sigma \mathbf{J}\boldsymbol{i}_s \tag{8}$$

and the back EMF corresponding to the current model

$$\hat{\boldsymbol{e}} = \hat{R}_R \boldsymbol{i}_s - (\hat{\alpha}\mathbf{I} - \hat{\omega}_m \mathbf{J})\hat{\boldsymbol{\psi}}_R \tag{9}$$

where $\hat{\alpha} = \hat{R}_\mathrm{R}/\hat{L}_\mathrm{M}$ is the estimate of the inverse rotor time constant. The estimated stator frequency is denoted by $\hat{\omega}_\mathrm{s}$. The classical approach of mimicking the current model at low speeds and the voltage model at high speeds is used, i.e. the rotor flux is estimated by

$$\frac{\mathrm{d}\hat{\boldsymbol{\psi}}_\mathrm{R}}{\mathrm{d}t} + \hat{\omega}_\mathrm{s}\mathbf{J}\hat{\boldsymbol{\psi}}_\mathrm{R} = \boldsymbol{e}' + \boldsymbol{K}(\hat{\boldsymbol{e}} - \boldsymbol{e}') \tag{10}$$

where the matrix $\boldsymbol{K}$ is the gain matrix. In order to achieve an inherently sensorless observer, the gain is selected as

$$\boldsymbol{K} = \frac{\boldsymbol{G}\hat{\boldsymbol{\psi}}_\mathrm{R}\hat{\boldsymbol{\psi}}_\mathrm{R}^\mathrm{T}}{\|\hat{\boldsymbol{\psi}}_\mathrm{R}\|} \tag{11}$$

where $\boldsymbol{G} = g_1\mathbf{I} + g_2\mathbf{J}$. Details on the selection of the gains g_1 and g_2 can be found in [11]. The speed estimate is obtained from

$$\hat{\omega}_\mathrm{m} = \hat{\omega}_\mathrm{s} - \frac{\hat{R}_\mathrm{R}\boldsymbol{i}_\mathrm{s}^\mathrm{T}\mathbf{J}\hat{\boldsymbol{\psi}}_\mathrm{R}}{\|\hat{\boldsymbol{\psi}}_\mathrm{R}\|^2} \tag{12}$$

IV. Inductance Adaptation

A. Adaptation of Inverse-Γ Inductances

The inductances L_M and L_σ vary due to the magnetic saturation and are, thus, dependent on the operating point. A straightforward way to take into account the magnetic saturation would be to apply adaptation laws based on the back EMF according to

$$\frac{\mathrm{d}\hat{L}_\mathrm{M}}{\mathrm{d}t} = \boldsymbol{k}_\mathrm{M}^\mathrm{T}(\hat{\boldsymbol{e}} - \boldsymbol{e}'), \quad \frac{\mathrm{d}\hat{L}_\sigma}{\mathrm{d}t} = \boldsymbol{k}_\sigma^\mathrm{T}(\hat{\boldsymbol{e}} - \boldsymbol{e}') \tag{13}$$

The gain vectors are denoted by $\boldsymbol{k}_\mathrm{M}$ and $\boldsymbol{k}_\sigma$, respectively. However, a continuous adaptation of the inductances might lead to poor dynamics. Furthermore, when no speed sensor is used, there is not enough information to simultaneously estimate the value of both the leakage inductance and the magnetizing inductance. As a change in the flux level leads to variations in both inductances, one of the estimates would be inaccurate if the adaptation laws above would be applied. Moreover, the estimate of L_σ is very sensitive to parameters errors when the identification is based on fundamental-wave operating-point data as in (13) [8].

B. Adaptation of Magnetic Saturation Function

Instead of adapting the inductances of the inverse-Γ model, the stator inductance function related to the Γ model is estimated. The function includes three parameters L_su, β, and S. For L_su and β, the adaptation laws

$$\frac{\mathrm{d}\hat{L}_\mathrm{su}}{\mathrm{d}t} = \boldsymbol{k}_\mathrm{L}^\mathrm{T}(\hat{\boldsymbol{e}} - \boldsymbol{e}') \tag{14}$$

$$\frac{\mathrm{d}\hat{\beta}}{\mathrm{d}t} = \boldsymbol{k}_\beta^\mathrm{T}(\hat{\boldsymbol{e}} - \boldsymbol{e}') \tag{15}$$

are proposed, where $\boldsymbol{k}_\mathrm{L}$ and $\boldsymbol{k}_\beta$ are the gain vectors for the parameters L_su and β, respectively. The parameter adaptation should not be coupled with the speed estimation. Therefore, the vectors are chosen as

$$\boldsymbol{k}_\mathrm{L} = k_\mathrm{L}\hat{\boldsymbol{\psi}}_\mathrm{R}/\|\hat{\boldsymbol{\psi}}_\mathrm{R}\| \tag{16}$$

$$\boldsymbol{k}_\beta = k_\beta\hat{\boldsymbol{\psi}}_\mathrm{R}/\|\hat{\boldsymbol{\psi}}_\mathrm{R}\| \tag{17}$$

where k_L and k_β are the adaptation gains. The stability analysis of the adaptation algorithm is presented in the Appendix. The resulting stability conditions for the adaptation gains are

$$k_\mathrm{L} < 0, \quad k_\beta > 0 \tag{18}$$

at stator frequencies above ω_Δ, cf. [11], which is the transition frequency between the current and voltage model in the observer. At lower speeds, it is advisable to turn the adaptation mechanism off.

At low flux levels, the stator inductance is approximately equal to L_su while the parameter β has basically no influence on the inductance. As both parameters cannot be estimated simultaneously, a natural choice is to estimate L_su at flux levels below a flux limit ψ_Δ, and β when the flux is higher than ψ_Δ. The exponent S could also be adapted in a similar manner. However, there is often a priori information about the value of S [9]. Furthermore, the implementation is simpler if the exponent is an integer. The parameter S is, therefore, kept constant. The derivative of the stator inductance with respect to S is

$$\frac{\mathrm{d}L_\mathrm{s}}{\mathrm{d}S} = -\frac{L_\mathrm{su}(\beta\psi_\mathrm{s})^S\ln(\beta\psi_\mathrm{s})}{[1 + (\beta\psi_\mathrm{s})^S]^2} \tag{19}$$

which equals zero when $\psi_\mathrm{s} = 1/\beta$. The parameter β should, thus, be estimated at this flux level to minimize the influence of a possibly erroneous value of S. After finding the values of L_su and β, the exponent S can be tuned based on the estimate of β. If the estimate of β varies as a function of the flux level, the value of S is probably inaccurate.

(The stator inductance could also be expressed as

$$L_\mathrm{s} = \frac{L_\mathrm{su}}{1 + \beta'\psi_\mathrm{s}^S} \tag{20}$$

The parameter β' should then be estimated as $\psi_\mathrm{s} = 1$ to minimize the influence of S.)

C. Leakage Inductance Identification

An estimate of the chord-slope leakage inductance is necessary in the implementation of the proposed stator inductance identification method. As previously mentioned, the leakage inductance estimate becomes very sensitive to parameter errors if the identification is based on fundamental-wave data. Therefore, high-frequency signal injections are used in order to identify the leakage inductance of the inverse-Γ model.

The principle of the identification method is the same as in [12], but here, a current signal is injected instead of a voltage signal. Due to magnetic saturation, the machine appears to be salient in transients. Therefore, the inductance obtained depends on the direction of the injected signal. As the direction that should be used to obtain the operating-point value of the inductance is not known in advance, the entire small-signal impedance matrix

$$\boldsymbol{Z}_\mathrm{s} = \begin{bmatrix} \underline{Z}_\mathrm{dd} & \underline{Z}_\mathrm{dq} \\ \underline{Z}_\mathrm{qd} & \underline{Z}_\mathrm{qq} \end{bmatrix} \tag{21}$$

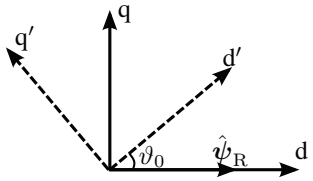

Fig. 4. Reference frames used in the identification of the leakage inductance. The inductance is first measured in the dq reference frame using signal injections. By means of a coordinate transformation, the inductance is calculated in the d′q′ reference frame as a function of ϑ_0.

is measured by injecting signals in two directions, first the d direction and then the q direction in a reference frame aligned with the estimated rotor flux. The current signal injected in the d direction is denoted by $\underline{I}_{\mathrm{d1}}$. The corresponding voltage signal in the d direction is denoted by $\underline{U}_{\mathrm{d1}}$ and in the q direction by $\underline{U}_{\mathrm{q1}}$. As the current in the d direction oscillates, the rotor flux also starts to oscillate. The torque controller tries to keep the torque constant, and a small deviation in the q direction current can, therefore, be observed. This deviation is denoted by $\underline{I}_{\mathrm{q1}}$. The relation between the currents and voltages can be described by

$$\begin{cases} \underline{Z}_{\mathrm{dd}}\underline{I}_{\mathrm{d1}} + \underline{Z}_{\mathrm{dq}}\underline{I}_{\mathrm{q1}} = \underline{U}_{\mathrm{d1}} \\ \underline{Z}_{\mathrm{qd}}\underline{I}_{\mathrm{q1}} + \underline{Z}_{\mathrm{qq}}\underline{I}_{\mathrm{q1}} = \underline{U}_{\mathrm{q1}} \end{cases} \tag{22}$$

Next, a current signal $\underline{I}_{\mathrm{q2}}$ is injected in the q direction. The corresponding voltage signals are denoted by $\underline{U}_{\mathrm{d2}}$ and $\underline{U}_{\mathrm{q2}}$ in the d and q direction, respectively, and the d direction current is denoted by $\underline{I}_{\mathrm{d2}}$. The following equations now hold

$$\begin{cases} \underline{Z}_{\mathrm{dd}}\underline{I}_{\mathrm{d2}} + \underline{Z}_{\mathrm{dq}}\underline{I}_{\mathrm{q2}} = \underline{U}_{\mathrm{d2}} \\ \underline{Z}_{\mathrm{qd}}\underline{I}_{\mathrm{d2}} + \underline{Z}_{\mathrm{qq}}\underline{I}_{\mathrm{q2}} = \underline{U}_{\mathrm{q2}} \end{cases} \tag{23}$$

The impedance matrix can be obtained by solving the two systems of equations in (22) and (23).

The leakage inductance seen in the rotor flux reference frame is

$$L_\sigma = \mathrm{Im}\{\underline{Z}_{\mathrm{qq}}\}/\omega_\mathrm{c} \tag{24}$$

where ω_c is the angular frequency of the injection signal. As previously stated, this value is not necessarily the desired operating-point inductance. In order to find the estimate for the chord-slope inductance, a coordinate transformation is applied. The inductance seen in a reference frame having the angle ϑ_0 in respect to the original rotor flux oriented reference frame can be written as

$$\begin{aligned} L_\sigma(\vartheta_0) = \mathrm{Im}\big\{&\underline{Z}_{\mathrm{dd}}\sin^2(\vartheta_0) + \underline{Z}_{\mathrm{qq}}\cos^2(\vartheta_0) \\ &- \big(\underline{Z}_{\mathrm{dq}} + \underline{Z}_{\mathrm{qd}}\big)\cos(\vartheta_0)\sin(\vartheta_0)\big\}/\omega_\mathrm{c} \end{aligned} \tag{25}$$

The angle ϑ_0 is illustrated in Fig. 4, and the value of this angle is varied in the range 0° to 180° when evaluating (25). As explained in [12], the maximum value of (25) corresponds to the desired leakage inductance.

V. Implementation

The observer is implemented in the estimated rotor-flux coordinates. The equations for the rotor flux and stator frequency become

$$\frac{\mathrm{d}\hat{\psi}_\mathrm{R}}{\mathrm{d}t} = e'_\mathrm{d} + g_1(\hat{e}_\mathrm{d} - e'_\mathrm{d}) \tag{26}$$

$$\hat{\omega}_\mathrm{s} = \frac{e'_\mathrm{q} + g_2(\hat{e}_\mathrm{d} - e'_\mathrm{d})}{\hat{\psi}_\mathrm{R}} \tag{27}$$

where

$$e'_\mathrm{d} = u_\mathrm{sd} - R_\mathrm{s}i_\mathrm{sd} - \hat{L}_\sigma\frac{\mathrm{d}i_\mathrm{sd}}{\mathrm{d}t} + \hat{\omega}_\mathrm{s}\hat{L}_\sigma i_\mathrm{sq} \tag{28a}$$

$$e'_\mathrm{q} = u_\mathrm{sq} - R_\mathrm{s}i_\mathrm{sq} - \hat{L}_\sigma\frac{\mathrm{d}i_\mathrm{sq}}{\mathrm{d}t} - \hat{\omega}_\mathrm{s}\hat{L}_\sigma i_\mathrm{sd} \tag{28b}$$

and

$$\hat{e}_\mathrm{d} = \hat{R}_\mathrm{R}(i_\mathrm{sd} - \hat{\psi}_\mathrm{R}/\hat{L}_\mathrm{M}) \tag{29}$$

The adaptation laws of L_su and β are

$$\frac{\mathrm{d}\hat{L}_\mathrm{su}}{\mathrm{d}t} = k_\mathrm{L}(\hat{e}_\mathrm{d} - e'_\mathrm{d}) \tag{30}$$

$$\frac{\mathrm{d}\hat{\beta}}{\mathrm{d}t} = k_\beta(\hat{e}_\mathrm{d} - e'_\mathrm{d}) \tag{31}$$

In the back-EMF equations (28) and (29), estimates of the parameters of the inverse-Γ model are used. The magnetizing inductance is calculated as $\hat{L}_\mathrm{M} = \hat{L}_\mathrm{s} - \hat{L}_\sigma$ where $\hat{L}_\sigma$ is the leakage inductance estimate obtained using signal injections. The stator inductance estimate $\hat{L}_\mathrm{s}$ is obtained from

$$\hat{L}_\mathrm{s} = \frac{\hat{L}_\mathrm{su}}{1 + (\hat{\beta}\hat{\psi}_\mathrm{s})^S} \tag{32}$$

where the stator flux amplitude is

$$\hat{\psi}_\mathrm{s} = \sqrt{(\hat{\psi}_\mathrm{R} + \hat{L}_\sigma i_\mathrm{sd})^2 + (\hat{L}_\sigma i_\mathrm{sq})^2} = f(\hat{\psi}_\mathrm{s}) \tag{33}$$

which is in fact itself a function of the stator flux amplitude. To overcome this problem, the stator flux is calculated based on data from the previous time step. The rotor resistance of the Γ model is assumed to be known, and the inverse-Γ rotor resistance is calculated using the model conversion given in (5). However, it is to be noted that the rotor resistance does not have any influence on the inductance estimate as the parameters are obtained in steady state.

VI. Simulation Results

Simulations were carried out in the MATLAB/Simulink environment. The data of a 2.2-kW induction machine with the rated voltage 400 V, rated current 5 A, rated speed 1436 r/min, and rated torque 14.6 Nm were used. The induction machine was implemented according to the Γ model. The following parameter values were used: $R_\mathrm{s} = 0.064$ p.u.; $R'_\mathrm{R} = 0.04$ p.u.; $L'_\sigma = 0.17$ p.u.; $L_\mathrm{su} = 2.31$ p.u.; $\beta = 0.87$ p.u.; and $S = 7$. The value of the flux limit ψ_Δ was 0.45 p.u., and the transition frequency ω_Δ was 0.25 p.u.

Fig. 5 shows the result of the adaptation as the value of the exponent S is known. At low flux levels, the value of

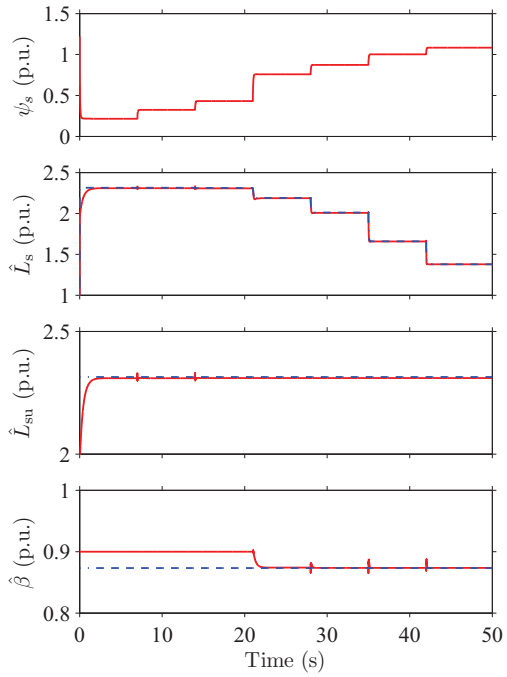

Fig. 5. Simulation results showing the adaptation of the saturation function parameters. The uppermost subplot shows the stator flux, the second subplot shows the estimated stator inductance, the third subplot shows the estimated value of L_{su} and the last subplot the estimated value of β. Estimated values are shown by red solid lines and actual values by blue dashed lines. The rotation frequency is 0.5 p.u. and the load torque is zero.

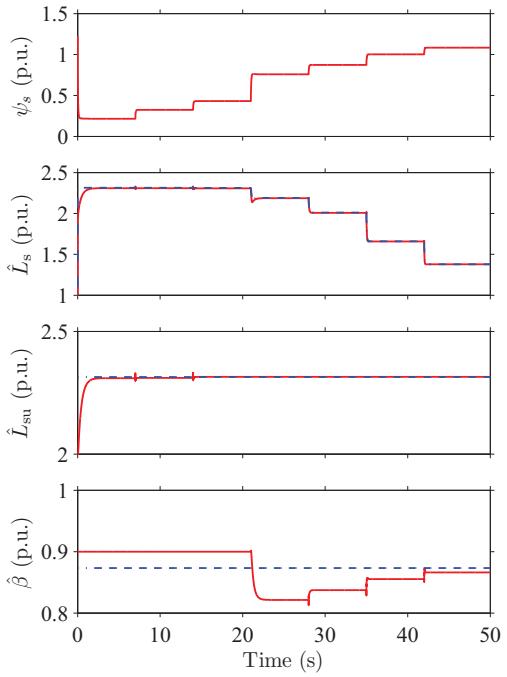

Fig. 6. Simulation results showing the adaptation of the saturation function parameters as the value of the exponent S deviates from the actual value. The rotation frequency is 0.5 p.u. and the load torque is zero.

$\hat{L}_{\mathrm{su}}$ converges rapidly to the actual value. When the flux is increased, the adaptation of L_{su} is turned off and the parameter β is adapted instead. As seen in the figure, the parameter β converges also very fast to the actual value. The resulting value of the estimated stator inductance is at all flux levels very close to the actual value. In Fig. 6, the situation is similar to that in Fig. 5, but the value of the exponent S is erroneously set to $S = 6$ instead of the actual value 7. At low flux levels, the influence of this error is very small, and the adaptation of L_{su} is as good as in the previous case. At higher flux levels, however, the error in S makes the estimate of β deviate from its actual value to compensate for the error in the exponent. Therefore, $\hat{\beta}$ varies as a function of the flux level and is no longer a constant. The resulting value of the estimated stator inductance is still very close to the actual inductance at all flux levels. However, if the value of β would be fixed to value obtained at the highest flux level in Fig. 6, the error in the stator inductance would be about 3% at rated flux.

VII. Experimental Results

Laboratory experiments were carried out on a 2.2-kW induction machine with skewed and closed rotor slots. The machine was fed by a frequency converter controlled by a dSPACE DS1103 PPC/DSP board. The rating was the same as in the simulations. A servo motor was used as a load.

Prior to the experiments, no-load tests were performed in order to obtain reference values for the parameters L_{su}, β, and S. The stator voltage and stator current were measured at different stator frequencies and voltage levels. The stator flux was evaluated at each operating point, and the stator inductance function (7) was fitted to the data. The measured inductance values as well as the results of the data fitting are shown in Fig. 3.

The performance of the adaptation algorithm is demonstrated at different speeds and loading conditions. Basically, it is enough to use only a few different flux levels, but here seven flux levels are used in order to get a good understanding of the adaptation method. Before each measurement sequence, the leakage inductance was identified using signal injections, and the value at each flux level was stored in a look-up table. The injection frequency $\omega_{\mathrm{c}} = 2\pi \cdot 60$ rad/s and the amplitude of the injected signal was 0.02 p.u.

Fig. 7 shows the experimental results at no load at the speed 0.9 p.u. The adaptation gains $k_{\mathrm{L}} = -5$ p.u. and $k_\beta = 1$ p.u. were used. The accuracy of the estimate of L_{su} is good as the rotor flux is 0.3 p.u. and 0.4 p.u., but at the lowest flux level 0.2 p.u., the estimate is slightly lower. A possible explanation to this is the presence of inaccuracies in the leakage inductance. Theoretically, the leakage inductance has no influence at no load, but, due to mechanical losses, a true no-load condition can not be achieved in practice. At very low flux levels, the q direction current becomes relatively large and the sensitivity to inaccuracies in the leakage inductance is high.

In Fig. 8, the results are shown as 10% of the rated load is applied while the rotation speed is 0.5 p.u. Due to the load, the estimate $\hat{L}_{\mathrm{su}}$ is now very sensitive to inaccuracies in the

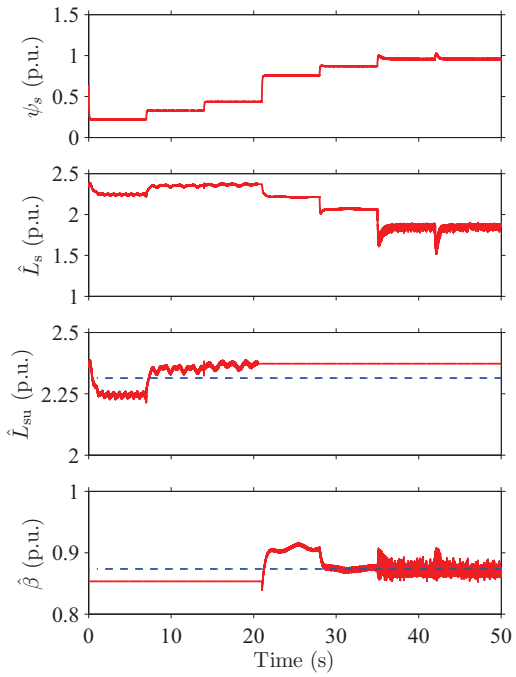

Fig. 7. Experimental results showing the adaptation of the saturation function parameters at no load. The rotation speed is 0.9 p.u. Estimated values are shown by red solid lines and the reference values obtained from no-load tests by blue dashed lines.

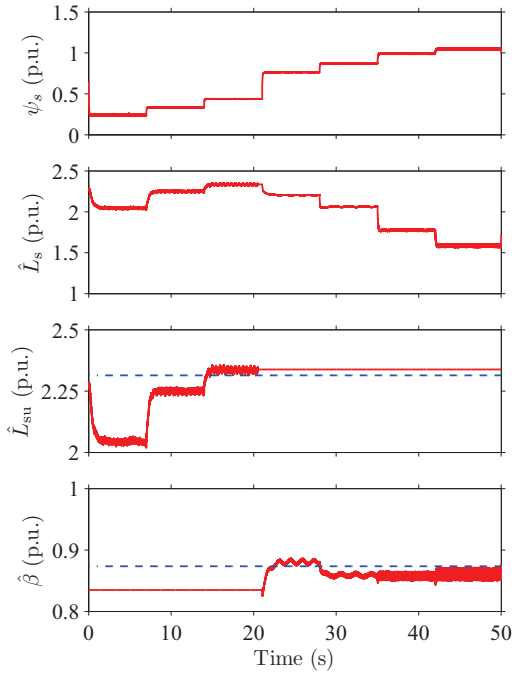

Fig. 8. Experimental results showing the adaptation of the saturation function parameters when a small load is applied. The rotation speed is 0.5 p.u. and the load torque is 10% of the rated load.

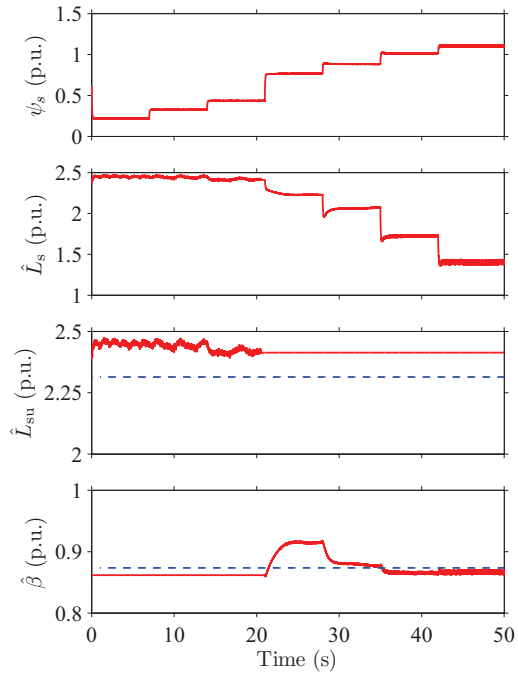

Fig. 9. Experimental results showing the adaptation of the saturation function parameters at the rotation speed 0.15 p.u.

leakage inductance at the lowest flux levels. As the flux is increased to 0.4 p.u., the estimate is, however, practically equal to the reference value. At higher flux levels, the influence of the load is negligible, and the accuracy of $\hat{\beta}$ is good.

The results at the rotation speed 0.15 p.u. are shown in Fig. 9. The adaptation gains were changed to $k_{\mathrm{L}} = -2$ p.u. and $k_\beta = 0.2$ p.u. in order to avoid large fluctuations in the estimates. The accuracy of the adaptation is poorer at low speeds, and the estimate of L_{su} is about 5% too large. Due to the high value of $\hat{L}_{\mathrm{su}}$, the estimate of $\hat{\beta}$ also increases as the rotor flux is about 0.7 p.u. At higher flux levels, the accuracy of $\hat{\beta}$ is still rather good, though. At this very low speed, the influence of the leakage inductance estimate is negligible at all flux levels.

Based on the laboratory experiments, it is seen that the most accurate results are obtained when the speed is high and the load is sufficiently low. Very low flux levels should be avoided when identifying the parameter L_{su} in order to minimise the influence of leakage inductance errors. The parameter β can successfully be identified if a flux level high enough is chosen. The minimum number of flux levels needed in the identification is two, and the entire saturation curve can, thus, be obtained in $10-15$ seconds.

VIII. Conclusion

Due to the magnetic saturation, the inductances in the induction machine model are dependent on the operating point. In this paper, the magnetic saturation of the stator inductance was modelled by a power function. Adaptation laws for the parameters of the function were proposed. The entire

magnetizing curve is obtained in a short time by applying two flux levels (one just below the saturation point and one close to the rated flux). No additional data fitting method is necessary as the power function parameters are directly identified. Simulations and laboratory experiments show that the parameters can be estimated with good accuracy. The leakage inductance is identified by signal injections prior to the identification of the stator inductance. In this manner, good results are obtained even in non-ideal no-load conditions.

APPENDIX
STABILITY ANALYSIS

Assuming constant L_M, L_σ and R_R, the nonlinear dynamics of the estimation error of L_su is

$$\frac{\mathrm{d}\tilde{L}_\mathrm{su}}{\mathrm{d}t} = \boldsymbol{k}_\mathrm{L}^\mathrm{T}(\hat{\boldsymbol{e}} - \boldsymbol{e}') \tag{34}$$

where $\tilde{L}_\mathrm{su} = \hat{L}_\mathrm{su} - L_\mathrm{su}$. The closed-loop system can be linearized as

$$\frac{\mathrm{d}}{\mathrm{d}t}\begin{bmatrix}\tilde{\boldsymbol{\psi}}_\mathrm{R}\\ \tilde{L}_\mathrm{su}\end{bmatrix} = \underbrace{\begin{bmatrix}\boldsymbol{A} & -B\boldsymbol{K}_0\boldsymbol{\psi}_\mathrm{R0}\\ -\boldsymbol{k}_\mathrm{L}^\mathrm{T}(\alpha\mathbf{I} - \omega_\mathrm{m0}\mathbf{J}) & -B\boldsymbol{k}_\mathrm{L}^\mathrm{T}\boldsymbol{\psi}_\mathrm{R0}\end{bmatrix}}_{\boldsymbol{A'}}\begin{bmatrix}\tilde{\boldsymbol{\psi}}_\mathrm{R}\\ \tilde{L}_\mathrm{su}\end{bmatrix} \tag{35}$$

where

$$\boldsymbol{A} = \begin{bmatrix}-g_{10}\alpha & -g_{10}\omega_\mathrm{m0} + \omega_\mathrm{s0}\\ -g_{20}\alpha - \omega_\mathrm{s0} & -g_{20}\omega_\mathrm{m0}\end{bmatrix} \tag{36}$$

$$B = -R_\mathrm{R}\frac{L_\mathrm{su}[1 + (\beta\psi_\mathrm{s0})^S] + 2L_\sigma[1 + (\beta\psi_\mathrm{s0})^S]^2}{L_\mathrm{su}^3} \tag{37}$$

The system matrix is

$$\boldsymbol{A'} = \begin{bmatrix}-g_{10}\alpha & -g_{10}\omega_\mathrm{m0} + \omega_\mathrm{s0} & -g_{10}B\psi_\mathrm{R0}\\ -g_{20}\alpha - \omega_\mathrm{s0} & -g_{20}\omega_\mathrm{m0} & -g_{20}B\psi_\mathrm{R0}\\ -k_\mathrm{L0}\alpha & -k_\mathrm{L0}\omega_\mathrm{m0} & -k_\mathrm{L0}B\psi_\mathrm{R0}\end{bmatrix} \tag{38}$$

and the stability criterion then are

$$Bk_\mathrm{L0}\psi_\mathrm{R0}\omega_\mathrm{s0}^2 > 0 \tag{39}$$

$$\begin{array}{rcll} k_\mathrm{L0} & < & 0, & \text{if } c_0 > \omega_\mathrm{s0}^2\\ k_\mathrm{L0} & > & -\frac{b_0 c_0}{B\psi_\mathrm{R0}(c_0 - \omega_\mathrm{s0}^2)}, & \text{if } c_0 < \omega_\mathrm{s0}^2 \end{array} \tag{40}$$

The parameters b_0 and c_0 are positive in all operating points, their definition can be found in [11].

The nonlinear dynamics of the estimation error of β is

$$\frac{\mathrm{d}\tilde{\beta}}{\mathrm{d}t} = \boldsymbol{k}_\beta^\mathrm{T}(\hat{\boldsymbol{e}} - \boldsymbol{e}') \tag{41}$$

The closed-loop system can be linearized as

$$\frac{\mathrm{d}}{\mathrm{d}t}\begin{bmatrix}\tilde{\boldsymbol{\psi}}_\mathrm{R}\\ \tilde{\beta}\end{bmatrix} = \underbrace{\begin{bmatrix}\boldsymbol{A} & -C\boldsymbol{K}_0\boldsymbol{\psi}_\mathrm{R0}\\ -\boldsymbol{k}_\beta^\mathrm{T}(\alpha\mathbf{I} - \omega_\mathrm{m0}\mathbf{J}) & -C\boldsymbol{k}_\beta^\mathrm{T}\boldsymbol{\psi}_\mathrm{R0}\end{bmatrix}}_{\boldsymbol{A''}}\begin{bmatrix}\tilde{\boldsymbol{\psi}}_\mathrm{R}\\ \tilde{\beta}\end{bmatrix} \tag{42}$$

where

$$C = R_\mathrm{R}S\beta^{S-1}\psi_\mathrm{s0}^S\frac{L_\mathrm{su} + 2L_\sigma[1 + (\beta\psi_\mathrm{s0})^S]}{L_\mathrm{su}^2} \tag{43}$$

$$\boldsymbol{A''} = \begin{bmatrix}-g_{10}\alpha & -g_{10}\omega_\mathrm{m0} + \omega_\mathrm{s0} & -g_{10}C\psi_\mathrm{R0}\\ -g_{20}\alpha - \omega_\mathrm{s0} & -g_{20}\omega_\mathrm{m0} & -g_{20}C\psi_\mathrm{R0}\\ -k_{\beta 0}\alpha & -k_{\beta 0}\omega_\mathrm{m0} & -k_{\beta 0}C\psi_\mathrm{R0}\end{bmatrix} \tag{44}$$

The stability criterion are

$$Ck_{\beta 0}\psi_\mathrm{R0}\omega_\mathrm{s0}^2 > 0 \tag{45}$$

$$\begin{array}{rcll} k_{\beta 0} & > & 0, & \text{if } c_0 > \omega_\mathrm{s0}^2\\ k_{\beta 0} & < & -\frac{b_0 c_0}{C\psi_\mathrm{R0}(c_0 - \omega_\mathrm{s0}^2)}, & \text{if } c_0 < \omega_\mathrm{s0}^2 \end{array} \tag{46}$$

ACKNOWLEDGEMENT

The authors gratefully acknowledge ABB Oy for the financial support.

REFERENCES

[1] A. Yahiaoui and F. Bouillault, "Saturation effect on the electromagnetic behaviour of an induction machine," *IEEE Trans. Magn.*, vol. 31, no. 3, pp. 2036–2039, May 1995.

[2] C. Gerada, K. Bradley, M. Sumner, and P. Sewell, "Evaluation and modelling of cross saturation due to leakage flux in vector controlled induction machines," in *Proc. IEEE IEMDC'03*, vol. 3, San Diego, CA, June 2003, pp. 1983–1989.

[3] H. Rasmussen, M. Knudsen, and M. Tønnes, "Parameter estimation of inverter and motor model at standstill using measured currents only," in *Proc. IEEE ISIE'96*, vol. 1, Warsaw, Poland, June 1996, pp. 331–336.

[4] M. R. H. Grotstollen, "Off-line identification of the electrical parameters of an industrial servo drive system," in *Conf. Rec. IEEE-IAS Annu. Meeting*, vol. 1, San Diego, California, Oct. 1996, pp. 213–220.

[5] N. R. Klaes, "Parameter identification of an induction machine with regard to dependencies on saturation," *IEEE Trans. Ind. Appl.*, vol. IA-29, no. 6, pp. 1135–1140, Nov./Dec. 1993.

[6] C. Sukhapap and S. Sangwongwanich, "Auto tuning of parameters and magnetization curve of an induction motor at standstill," in *Proc. IEEE ICIT'02*, vol. 1, Bangkok, Thailand, Dec. 2002, pp. 101–106.

[7] E. Levi and S. N. Vukosavic, "Identification of the magnetising curve during commissioning of a rotor flux oriented induction machine," vol. 146, no. 6, pp. 685–693, Nov. 1999.

[8] J. L. Zamora and A. García-Cerrada, "Online estimation of the stator parameters in an induction motor using only voltage and current measurements," *IEEE Trans. Ind. Appl.*, vol. 36, no. 3, pp. 805–816, May/June 2000.

[9] H. C. J. de Jong, "Saturation in electrical machines," in *Proc. ICEM'80*, vol. 3, Athens, Greece, Sept. 1980, pp. 1545–1552.

[10] T. Tuovinen, M. Hinkkanen, and J. Luomi, "Modeling of saturation due to main and leakage flux interaction in induction machines," *IEEE Trans. Ind. Appl.*, vol. 46, no. 3, pp. 937–945, May/June 2010.

[11] M. Hinkkanen, L. Harnefors, and J. Luomi, "Reduced-order flux observers with stator-resistance adaptation for speed-sensorless induction motor drives," *IEEE Trans. Power Electronics*, vol. 25, no. 5, pp. 1173–1183, May 2010.

[12] M. Ranta, M. Hinkkanen, and J. Luomi, "Inductance identification of an induction machine taking load-dependent saturation into account," in *Proc. ICEM'08*, Vilamoura, Portugal, Sept. 2008.

BIOGRAPHIES

Mikaela Ranta received the M.Sc.(Eng.) degree from Helsinki University of Technology, Espoo, Finland, in 2006. Since 2006, she has been with Aalto University, Espoo, Finland, where she is currently a Research Scientist in the School of Electrical Engineering. Her main research interest is the modeling of electric machines.

Marko Hinkkanen (M06) received the M.Sc.(Eng.) and D.Sc.(Tech.) degrees from Helsinki University of Technology, Espoo, Finland, in 2000 and 2004, respectively. Since 2000, he has been with Helsinki University of Technology (part of Aalto University, Espoo, Finland, since 2010). He is currently an Adjunct Professor in the School of Electrical Engineering, Aalto University. His research interests include electric drives and electric machines.